ELECTROCHEMICAL DEPOSITION OF COBALT ON GOLD STUDIED WITH SCANNING TUNNELING MICROSCOPE

Iwona Flis-Kabulska[1)] and Margitta Uhlemann[2)]

[1)] *Institute of Physical Chemistry of PAS, Warsaw, Poland*
[2)] *Institute of Solid State and Materials Research, Dresden, Germany*

Abstract

Cobalt was electrodeposited from the $CoSO_4 + H_2SO_4$ solution on evaporated gold film and its topography was examined with Electrochemical Scanning Tunneling Microscope (ECSTM). Deposition of Co was observed at potentials nobler than the equilibrium potential in the solution used ($E^o_{Co/Co^{2+}} = -1.03$ V(MSE) = –0.35 V(NHE)), denoting the occurrence of the underpotential deposition (UPD). At the potential of –0.78 V(MSE) cobalt islands of atomic size were formed, at –0.88 V the islands increased in number and they started to grow, and at –0.98 V larger islands were formed. It was found that the UPD cobalt significantly hindered the hydrogen evolution reaction. It is supposed that the electrochemical deposition of cobalt proceeds similarly as the deposition in UHV, first by the deposition of one or two monolayers, and then the growth of 3D islands. The presence of monolayers was deduced from the hindrance of the HER.

Introduction

Cobalt is an important component of bimetallic surface layers [1]. New bimetallic materials have unique physical and chemical properties and can find applications in the areas of catalysis, electrochemistry and microelectronics. This metal can also constitute multi-layered materials composed of several hundred metallic nanolayers, alternately magnetic (e.g. ferromagnetic Co) and nonmagnetic materials [2]. Such materials can serve as devices for data storage or as magnetic sensors; owing to high hardness and low friction, they can be used for engineering parts demanding a high resistance to tribological impact [2].

In these materials, nanolayers are usually deposited by molecular beam epitaxy (MBE), thermal evaporation or sputtering [2,3,4,5,6], but efforts are being made to replace these techniques by electrochemical methods. The latter methods are simpler and provide a possibility of a control of an amount of the deposited materials [2,5,7].

In the present work the electrochemical deposition of cobalt was examined. Cobalt has a great potential for application due to its magnetic, catalytic and optical properties [8]. Properties of the material with deposited thin film of cobalt depend on the substrate, deposition method and conditions of the process [9,10]. The underpotential deposition (UPD) of cobalt in basic solutions results in the formation of two-dimensional cobalt nuclei and can be considered as the initial stage of the overpotential deposition (OPD) when three-dimensional cobalt nuclei are formed [8,11].

In the present work, early stages of cobalt electrodeposition were examined on the gold surface in the acidic sulphate solution with Electrochemical Scanning Tunneling Microscope (ECSTM).

Experimental

Topography of Co electrodeposited on gold was investigated *in situ* with the ECSTM Molecular Imaging. STM tips were made of PtIr wire etched in 30% $CuCl_2$ and isolated with Apiezon Wax; a PtIr wire was also used for a counter electrode and for a reference electrode in the electrochemical cell of the microscope.

The working gold electrode was of polycrystalline gold evaporated on glass; before the experiment it was flame annealed in a reducing flame to obtain reconstructed Au (111) surface [12,13,14]. The electrodeposition was conducted in a solution of 3 mM $CoSO_4$ + 0.5 mM H_2SO_4 at pH 3.0.

Electrochemical measurements were also performed on gold in form of a sheet of bulk metal in a conventional electrochemical cell, in the solutions: 0.5 mM H_2SO_4, 3 mM $CoSO_4$+ 0.5 mM H_2SO_4, and 14.9 mM $CoSO_4$ + 0.5 mM H_2SO_4. In these measurements, potentials were measured and reported in this paper against mercury sulphate electrode $Hg|Hg_2SO_4|$0.5 mM H_2SO_4 (designated here as MSE) (E^o (MSE) = +0.68 V(NHE)). Voltammetric sweeps were measured at the potential scan rate of 50 mV s^{-1} after a 10-min holding at the open circuit potential. Polarisation curves were measured at the potential scan rate of 1 mV s^{-1} after holding at cathodic potentials for 10 min. The measurements were made at ambient temperature in non-deaerated solutions.

Results

Electrochemical measurements

Typical current-voltage curves on gold in the H_2SO_4 solution without and with Co^{2+} cations are shown in Fig. 1. In the figure there are marked electrochemical reactions, and the equilibrium potentials in the solution used (pH 3.0, 3mM $CoSO_4$) for the hydrogen evolution reaction (HER) (E^o_{H/H^+} = –0.857 V(MSE)) and for the Co/Co^{2+} couple ($E^o_{Co/Co^{2+}}$ = –1.031 V(MSE)).

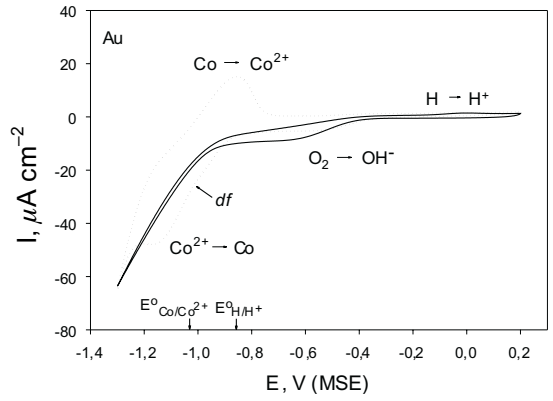

Figure 1. Cyclic voltammograms on Au in 0.5 mM H_2SO_4 (—) and in 3 mM $CoSO_4$ + 0.5 mM H_2SO_4 (.....) (forth scans; scan rate 50 mV s^{-1}; *df* indicates a deflection).

In the solution with Co^{2+}, in the cathodic sweep the currents at the potentials below E^o_{H/H^+} were higher than those in the Co^{2+}-free solution, demonstrating the occurrence both of the $H^+ \Rightarrow H$ and $Co^{2+} \Rightarrow Co$ reactions. It is noted that the increased current in this solution started at potentials nobler than $E^o_{Co/Co^{2+}}$; this indicates the UPD of Co. A small deflection (*df*) on the curve in the solution with Co^{2+} suggests a hindrance of HER caused by the deposited cobalt. A plateau at more cathodic potentials is evidently a limiting current due to the diffusion of Co^{2+} cations. In the anodic sweep, cathodic currents at potentials to about –1.15 V(MSE) were lower than those in the solution without Co^{2+}. This indicates that the HER on the deposited cobalt was slower than that on gold. Evidently, cobalt increases the overpotential of hydrogen evolution relative to gold, similarly as do it iron and nickel [15] belonging to the same VIII group of the periodic table.

Anodic currents at more positive potentials were associated with the anodic oxidation of the deposited cobalt.

In order to find out, whether the UPD cobalt can be detected by a current of its anodic oxidation, the electrodeposition was conducted at various potentials for 10 min, and subsequently anodic sweeps were performed at a scan rate of 1 mV s^{1-}. Fig. 2 shows anodic sweeps after polarisation at potentials below $E^{o}_{Co/Co^{2+}}$. Only the polarisation at –1.2 V resulted in a distinct anodic current of the $Co \Rightarrow Co^{2+}$ reaction between about –0.9 V and –0.75 V, manifesting the deposition of cobalt. The polarisation at –1.17 V and –1.15 V did not give any meaningful decrease of the cathodic current which could be ascribed to the $Co \Rightarrow Co^{2+}$ reaction. This indicates that small amounts of Co cannot be determined by anodic sweeps, and thus these measurements are not sensitive enough to detect the UPD cobalt.

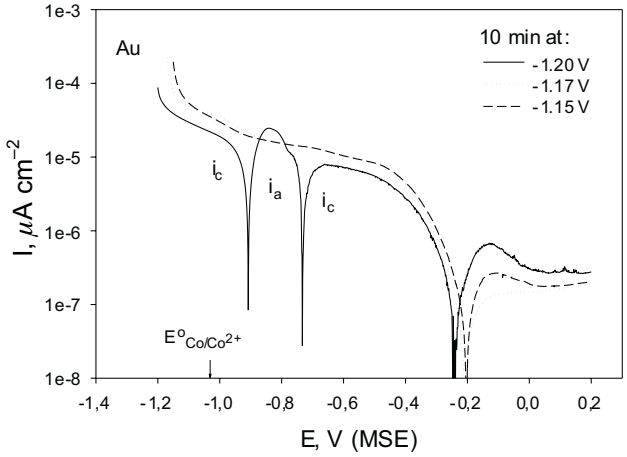

Figure 2. Anodic sweeps in 3 mM $CoSO_4$ + 0.5 mM H_2SO_4 after 10-min holding at potentials –1.20 V, –1.17 V and –1.15 V (MSE). Scan rate 1mV s^{-1}; i_c, i_a are cathodic and anodic currents, respectively.

However, the presence of the UPD Co can be deduced from the HER current. As seen in Figs. 1 and 2, the HER current decreases after deposition of Co. A decrease in the HER current was also observed for the UPD Co; Fig. 3 shows that after holding in the solution with Co^{2+} for 10 min at the potential of –1.00 V, the cathodic current was lower than that in the Co^{2+}-free solution. In addition, a distinct anodic peak of the $H \Rightarrow H^{+}$ reaction appeared in the Co^{2+}-free solution, whereas it did not occur in the solution with Co^{2+}. Evidently, small amounts of the UPD Co effectively reduced the HER and accordingly, the amount of adsorbed hydrogen which is manifested by the anodic peak $H \Rightarrow H^{+}$.

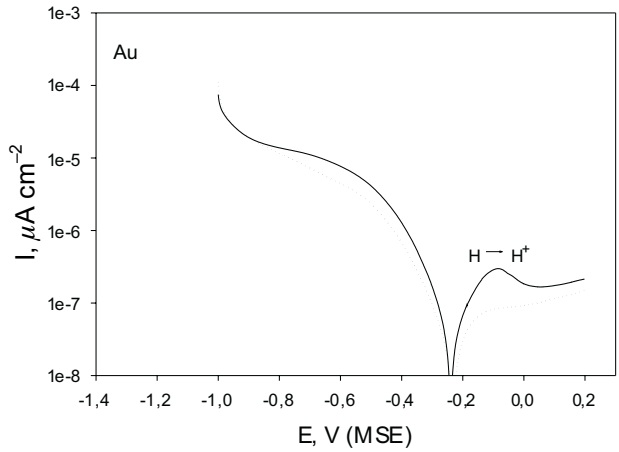

Figure 3. Anodic sweeps in 0.5 mM H_2SO_4 (——) and in 14.9 mM $CoSO_4$ + 0.5 mM H_2SO_4 (.....) after 10-min holding at the potential of –1.00 V (MSE). Scan rate 1mV s^{-1}.

STM study

Surface of gold after flame annealing is shown in Fig. 4. Typical for such a surface are flat terraces of the monoatomic height of about 0.2–0.3 nm. Flame annealing of gold yields the well defined surface with the orientation of (111) [12,13,14].

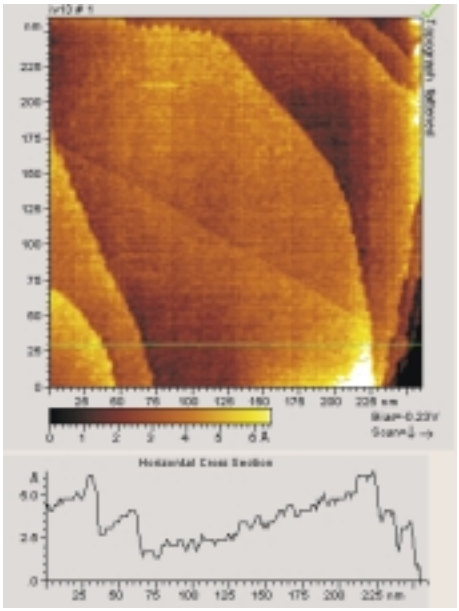

Figure 4. In situ STM of flame annealed gold. Profile shows that steps at the terraces are about 0.2–0.3 nm high (bias –0.23 V).

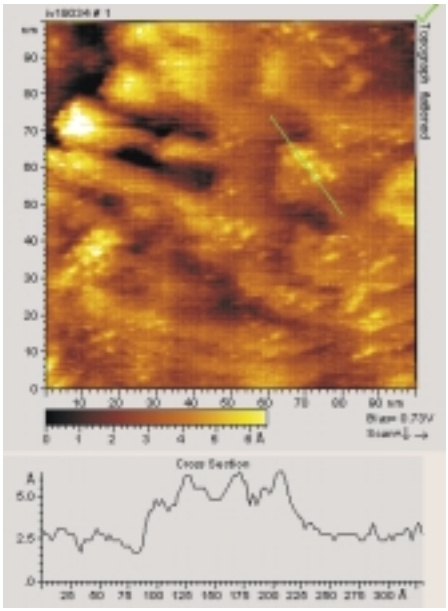

Figure 5. Cobalt islands (seen as dots) on gold after a 17-min polarisation at –0.78 V (MSE) in 3 mM $CoSO_4$ + 0.5 mM H_2SO_4 (bias +0.73 V).

Electrodeposition of cobalt was conducted in the 3 mM $CoSO_4$ + 0.5 mM H_2SO_4. No deposits were detected at the potential of –0.73 V, but they were seen at –0.78 V (MSE). Fig. 5 presents an image of gold with Co deposits in form of small islands, formed after a polarisation at –0.78 V for 17 min. The islands were monoatomic in height and about 1–2 nm wide. They were agglomerated in clusters or formed linear arrays. They formed in random; any preferred sites of deposition, such as kinks, were not observed.

The same growth mode was observed at the potential of –0.88 V. Small islands appeared after a 1-min polarisation. Their number increased with time as shown in Fig. 6; initially their number

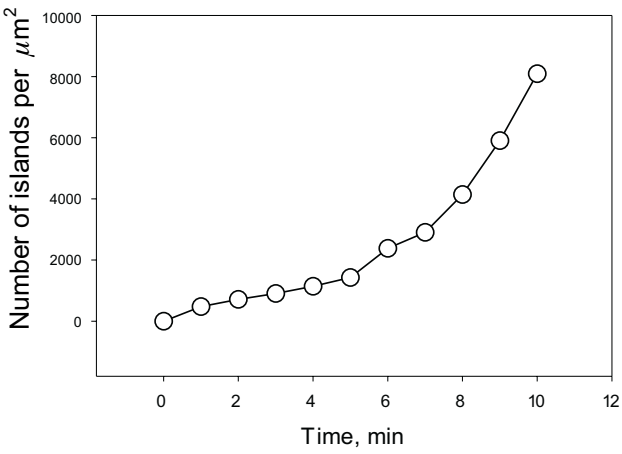

Figure 6. Number of islands of cobalt on gold as a function of the polarisation time at –0.88V(MSE).

increased linearly with time, but after about 5 min. the formation of the islands was considerably accelerated. The size of these deposits appeared to remain unchanged, suggesting that they are the nucleation centres. At more negative potentials the nucleation centres were larger; *e.g*. after 1 min at –0.98 V (MSE) they were up to about 3 nm wide and about 1 nm high, but their number was similar as that at -0.88 V. This indicates a faster growth of the cobalt islands at more negative potentials.

Potential sweeps from the electrochemical deposition to anodic oxidation usually did not result in the disappearance of the deposited islands. Fig. 7 shows the images at –0.88 V and after a potential shift to +0.27 V. At the latter potential the islands did not disappear; on the contrary, they grew in size and also in the number. This potential is much nobler than the potential of the anodic oxidation of the deposited cobalt (Fig. 2), therefore, these islands might be the products of the anodic oxidation of cobalt - its sulphate salts and/or oxides.

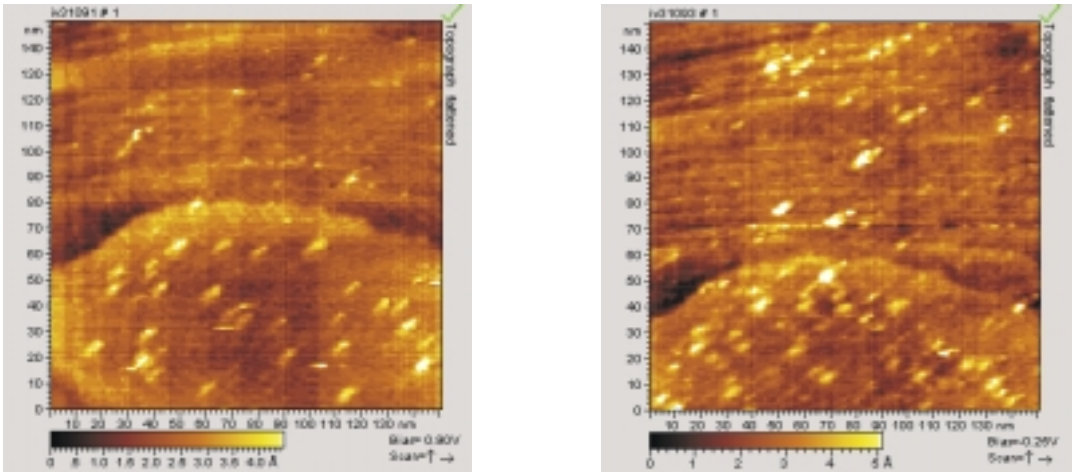

Figure 7. In-situ STM images in the system of Au/3 mM $CoSO_4$ + 0.5 mM H_2SO_4 at (a) –0.88 V after 6 min (formation of Co islands) (bias +0.90 V), and (b) after a sweep to +0.27 V (bias –0.25 V) (the islands did not disappear at the noble potenti

Discussion

This STM study revealed the underpotential deposition of cobalt in form of islands which for the high underpotential ΔE ($E - E^{o}_{Co/Co^{2+}}$) were of about an atomic size. Probably, they are adsorbed atoms Co_{ads}. For smaller ΔE these islands were larger, indicating the formation of 3D islands.

The study of the deposition of cobalt on gold in UHV [1] have shown that cobalt nucleates initially as an admetal at the kinks of gold, then it forms triangular 2D islands which spread forming the first layer of adsorbate. Because of a misfit of adatom to the substrate, the first layer grows as a pseudomorphic layer. Subsequent layers are closer to the crystal structure of the admetal (cobalt). Usually in the case of the high misfit, the epitaxial growth is suppressed in favour of the 3D islands. The deposition of cobalt on gold would thus proceed first by the formation of one or two monolayers, and then by the growth of 3D islands. This is the Stranski-Krastanov growth mode of the 3D metal island formation on top of predeposited 2D Me_{ads} overlayers on the substrate [16].

In the present work only the 3D islands of cobalt were observed, but no 2D monolayers. Nevertheless, this does not exclude its formation. Namely, their presence might be deduced from the hindrance of the HER; such a hindrance is indicated by a small deflection on the cathodic scan

of the voltammetric cycle at the potential of about –0.95 V (Fig. 1). On the basis of these results it can be supposed that the UPD of cobalt on gold proceeds by the metal layer-by-layer growth mode.

Conclusions

Electrochemical measurements and *in situ* STM studies of the Au/Co^{2+} (pH 3.0) system have shown the following:

- the underpotential deposition (UPD) of cobalt on gold occurs in the form of islands which are of the atomic size at high underpotentials (ΔE) or they are larger at low ΔE;
- the UPD cobalt hinders the hydrogen evolution reaction (HER), and this effect can be used for a indirect detection of the cobalt deposition;
- cobalt islands after anodic oxidation have similar STM image as prior to the oxidation, but islands of the oxidation products are larger;
- it is supposed that the electrochemical deposition of cobalt proceeds similarly as the deposition in UHV, first by the deposition of one or two monolayers, and then the growth of 3D islands. The presence of monolayers was deduced from the hindrance of the HER.

Acknowledgment

Authors express their thanks to Professor Janusz Flis for the discussions and to Monika Kuczyńska, MSc, for her help in electrochemical measurements.

References

1. J.A. Rodriguez, *Surf.Sci.Reports,* **24**, 223 (1996).
2. A. Banaszkiewicz, *Ochrona przed korozją*, **11**, 305 (2002).
3. D. Awschalom, J. Baumberg, *Physics Worl,* **6**, 31 (1993).
4. D. Tench, J. White, *J. Electrochem. Soc.,* **137**, 10 (1990).
5. N. Lebbad, J. Voiron, B. Nguyen, E. Chainet, *Thin Solid Films*, **275**, 216 (1996).
6. S. Jomni, N. Mliki, R. Belhi, K. Abdelmoula, M. Ayadi, G. Ninoul, *Thin Solid Films*, **370**, 186 (2000).
7. J.A. Switzer, K.G. Sheppard, *The Electrochemical Society Interface*, Summer (1995).
8. L.H. Mendoz-Huizar, J. Robles, M. Palomar-Pardavē, *J. Electroanal. Chem.,* **521**, 95 (2002).
9. V. Repain, J.M. Berroir, S. Rousset, J. Lecoeur, *Surf. Sci.* **447**, L152 (2000).
10. K.G. Mishra, P. Singh, D.M. Muir, *Hydrometallurgy,* **65**, 97 (2002).
11. L.H. Mendoz-Huizar, J. Robles, M. Palomar-Pardavç, *J. Electroanal. Chem.,* **545**, 39 (2003).
12. R.J. Nichols, E. Bunge, H. Meyer, H. Baumgärtel, *Surf. Sci.,* **335,** 110 (1995).
13. J. Clavilier, R. Faure, G. Guinet, R. Durand, *J. Electroanal. Chem.,* **107,** 205 (1980).
14. W. Haiss, D. Lackey, J.K. Sass, K.H. Besocke, *J. Chem. Phys.,* **95,** 2193 (1991).
15. P. Rüetschi, P. Delahay, *J. Chem. Soc.* **23**, 195 (1955).
16. G. Staikov, W.J. Lorenz, in *Electrochemical Nanotechnology* (Ed. W.J. Lorenz and W. Plieth), p. 13. Wiley-VCH, Weinheim (1998).